Cell. Mol. Life Sci. (2018) 75:547–561
DOI 10.1007/s00018-017-2641-7

Cellular and Molecular Life Sciences

ORIGINAL ARTICLE

Platelet-derived growth factor receptor beta identifies mesenchymal stem cells with enhanced engraftment to tissue injury and pro-angiogenic property

Shan Wang[1,2] · Miaohua Mo[1,2] · Jinmei Wang[2] · Sobia Sadia[1,2] · Bihua Shi[3] · Xiaobing Fu[4,5] · Lin Yu[6] · Edward E. Tredget[7] · Yaojiong Wu[2,3]

Received: 14 June 2017 / Revised: 20 August 2017 / Accepted: 31 August 2017 / Published online: 19 September 2017

Abstract Mesenchymal stem cells (MSCs) are heterogeneous likely consisting of subpopulations with various therapeutic potentials. Here we attempted to acquire a subset of MSCs with enhanced effect in wound healing. We found that human placental MSCs expressing platelet-derived growth factor (PDGF) receptor (PDGFR)-β exhibited greater proliferation rates and generated more colony-forming unit-fibroblast (CFU-F), compared to PDGFR-β$^-$ MSCs. Notably, PDGFR-β$^+$ MSCs expressed higher levels of pro-angiogenic factors such as Ang1, Ang2, VEGF, bFGF and PDGF. When 10^6 GFP-expressing MSCs were topically applied into excisional wounds in mice, PDGFR-β$^+$ MSCs actively incorporated into the wound tissue, resulting in enhanced engraftment ($3.92 \pm 0.31 \times 10^5$ remained in wound by 7 days) and accelerated wound closure; meanwhile, PDGFR-β$^-$ MSCs tended to remain on the top of the wound bed with significantly fewer cells ($2.46 \pm 0.26 \times 10^5$) engrafted into the wound, suggesting enhanced chemotactic migration and engraftment of PDGFR-β$^+$ MSCs into the wound. Real-Time PCR and immunostain analyses revealed that the expression of PDGF-B was upregulated after wounding; transwell migration assay showed that PDGFR-β$^+$ MSCs migrated eightfold more than PDGFR-β$^-$ MSCs toward PDGF-BB. Intriguingly, PDGFR-β$^+$ MSC-treated wounds showed significantly enhanced angiogenesis compared to PDGFR-β$^-$ MSC- or vehicle-treated wounds. Thus, our results indicate that PDGFR-β identifies a subset of MSCs with enhanced chemotactic migration to wound injury and effect in promoting angiogenesis and wound healing, implying a greater therapeutic potential for certain diseases.

Keywords Mesenchymal stem cells · Subpopulation · PDGFR-β (CD140b) · Angiogenesis · Wound healing

Shan Wang and Miaohua Mo contributed equally to this work.

Electronic supplementary material The online version of this article (doi:10.1007/s00018-017-2641-7) contains supplementary material, which is available to authorized users.

✉ Yaojiong Wu
wu.yaojiong@sz.tsinghua.edu.cn

1 School of Life Sciences, Tsinghua University, Beijing, China

2 The Shenzhen Key Laboratory of Health Sciences and Technology, Graduate School at Shenzhen, Tsinghua University, L406A, Tsinghua Campus, The University Town, Shenzhen 518055, China

3 Tsinghua-Berkeley Shenzhen Institute (TBSI), Tsinghua University, Shenzhen, China

4 Wound Healing and Cell Biology Laboratory, Institute of Basic Medical Science, Chinese PLA General Hospital, Beijing, China

5 Stem Cell and Tissue Regeneration Laboratory, The First Affiliated Hospital, General Hospital of PLA, Beijing, China

6 Peking University Shenzhen Hospital, Shenzhen Key Laboratory of Gynecological Diagnostic Technology Research, Shenzhen, China

7 Wound Healing Research Group, Department of Surgery, University of Alberta, Edmonton, AB, Canada

Introduction

Mesenchymal stem cells (MSCs) have been considered as an ideal source for cell and gene therapy strategies [1, 2]. However, MSCs obtained in current isolation and cultivation regimes are heterogeneous, and often represent a mixture of phenotypically, functionally and biochemically diverse cells with distinct morphologic and functional characteristics [3, 4]. This often leads to incomparable experimental results. The lack of a specific cell surface marker for prospective isolation of MSCs makes the isolation and identification of the cells difficult and inconsistent.

Platelet-derived growth factor (PDGF) receptor beta (PDGFR-β), also known as CD140b, is expressed on perivascular mesenchymal cells including pericytes and endothelial progenitor cells. Previous studies indicate that PDGFR-β signaling plays a key role in vascular mural cell formation. Lack of PDGFR-β leads to reduced vascular smooth muscle cell/pericyte proliferation and migration, and affects embryonic blood vessel formation in mice [5]. In addition, it has been demonstrated that PDGFR-β is involved in the recruitment and proliferation of pericytes during the remodeling phase of wound healing [6]. Recent studies suggest that PDGFR-β-mediated signaling is a potent regulator of MSC function, which appears to promote the proliferation and migration but suppress osteogenic differentiation of the cells [7]. In addition, sorted PDGFR-β^+ MSCs expressed some genes normally expressed in smooth muscle cells such as α-SMA, SM22, MYH11 [8], but direct contribution of MSCs to vascular smooth muscle cells is lacking.

Optimum healing of a cutaneous wound requires a well-orchestrated integration of the complex biological and molecular events of cell migration and proliferation and extracellular matrix (ECM) deposition, angiogenesis, and remodeling [9, 10]. However, this orderly progression of the healing process is impaired in many chronic diseases, including diabetes [9]. Up to almost 50% of chronic wounds that have been present for more than a year remain resistant to treatment [9, 11, 12]. Neovascularization is a crucial step in the wound healing process [9, 10, 13]. The formation of new blood vessels is necessary to sustain the newly formed granulation tissue and the survival of keratinocytes. A large number of animal studies and several preliminary clinical observations indicate that MSCs enhance wound healing by promoting angiogenesis, decreasing inflammation, and reducing scarring [12, 14–17]. However, the heterogeneity in MSC preparations has been a significant limitation for the clinical application of the cells [3, 12, 16].

In this study, we showed that PDGFR-β identified a subset of MSCs with enhanced effect in promoting angiogenesis and wound healing, thus facilitating the isolation of uniform MSCs for repetitive effects in promoting wound repair.

Materials and methods

Mice

BALB/C mice (7–8 weeks old) and athymic nu/nu mice (6 weeks old) were purchased from the Laboratory Animal Centre, Guangdong province, People's Republic of China (http://gdmlac.com.cn). All animals were maintained in a temperature-controlled environment (20 ± 1 °C) with access to food and water throughout the experiment. All procedures were performed with the approval of the Animal Ethics Committee of Tsinghua University. Tie2-GFP mice which expressed green fluorescent protein (GFP) under the direction of the endothelial-specific receptor tyrosine kinase (*Tek*, formerly, *Tie2*) promoter were obtained from the Jackson Laboratory.

Cell culture

Mesenchymal stem cells were isolated from human placenta as described previously [18, 19]. Briefly, term (38–40 weeks gestation) placentas from healthy donors were harvested with written informed consent and the procedure was approved by the Ethics Committee of Peking University Shenzhen Hospital. The placental tissue was washed several times with cold phosphate-buffered saline (PBS) and then mechanically minced and enzymatically digested with 0.25% trypsin–EDTA for 30 min at 37 °C in a water bath. The digest was subsequently filtered, pelleted, and resuspended in a growth medium consisting of Dulbecco's modified Eagle's medium (DMEM; Gibco-Invitrogen, http://www.invitrogen.com), 10% fetal bovine serum (FBS; Gibco-Invitrogen), and antibiotics. Cells were seeded on tissue culture dishes. 24 h later, medium was changed to remove cells that had not attached to the plate. Subsequently medium was replaced every 2 days to allow cell colonies to grow to reach 80% confluence. Cells were then subcultured after trypsinization. Cells derived from four donors were used for experiments. To track MSCs in vivo, the cells were labeled with lentiviral GFP.

Flow cytometry

Mesenchymal stem cells were analyzed by flow cytometry as previously described [19]. Briefly, cells were suspended in PBS containing 1% bovine serum albumin (BSA) at 10^6 per ml. 100-µl cell aliquots were incubated with anti-human PDGFR-β phycoerythrin (PE) (Biolegend, http://www.biolegend.com), anti-biotin PDGFR-β antibody (Miltenyi Biotec, Germany, http://www.miltenyibiotec.com) or control isotype IgG on ice for 30 min. 10,000 events were analyzed by flow cytometry (Becton-Dickinson, http://www.bd.com) using Cell Quest software.

Cell sorting

Cultured MSCs were prepared as single cell suspensions and sorted into PDGFR-β$^+$ and PDGFR-β$^-$ cells by fluorescence-activated cell sorting (FACS) using a FACS Aria II 5-LASER sorter system (BD Bioscience). Sorted cells were analyzed either immediately or after an indicated period of culture. Alternatively, MSCs were sorted into PDGFR-β$^+$ and PDGFR-β$^-$ cells by magnetic-activated cell sorting (MACS) using magnetic beads (Miltenyi Biotec) coated with anti-human PDGFR-β antibody.

MSC proliferation and CFU-F assay

Mesenchymal stem cell proliferation was examined by counting the cell number in each passage for seven successive passages. Colony-forming unit-fibroblast (CFU-F) assay was performed as previously described with minor modifications [20]. PDGFR-β$^+$ and PDGFR-β$^-$ MSCs at passage 4 were seeded in six-well culture plate at a density of 200 cells per well in the growth medium which was changed every 3 days. After 14 days of culture, the cells were fixed with 4% paraformaldehyde (PFA, Sigma-Aldrich, http://www.sigmaaldrich.com) and stained with 0.1% crystal violet solution (Sigma-Aldrich). The number of colonies (diameter ≥2 mm) was counted.

MSC differentiation assays

Mesenchymal stem cells were incubated to differentiate into adipocytes, osteoblasts and chondrocytes in corresponding induction medium as previously described [14, 18, 21].

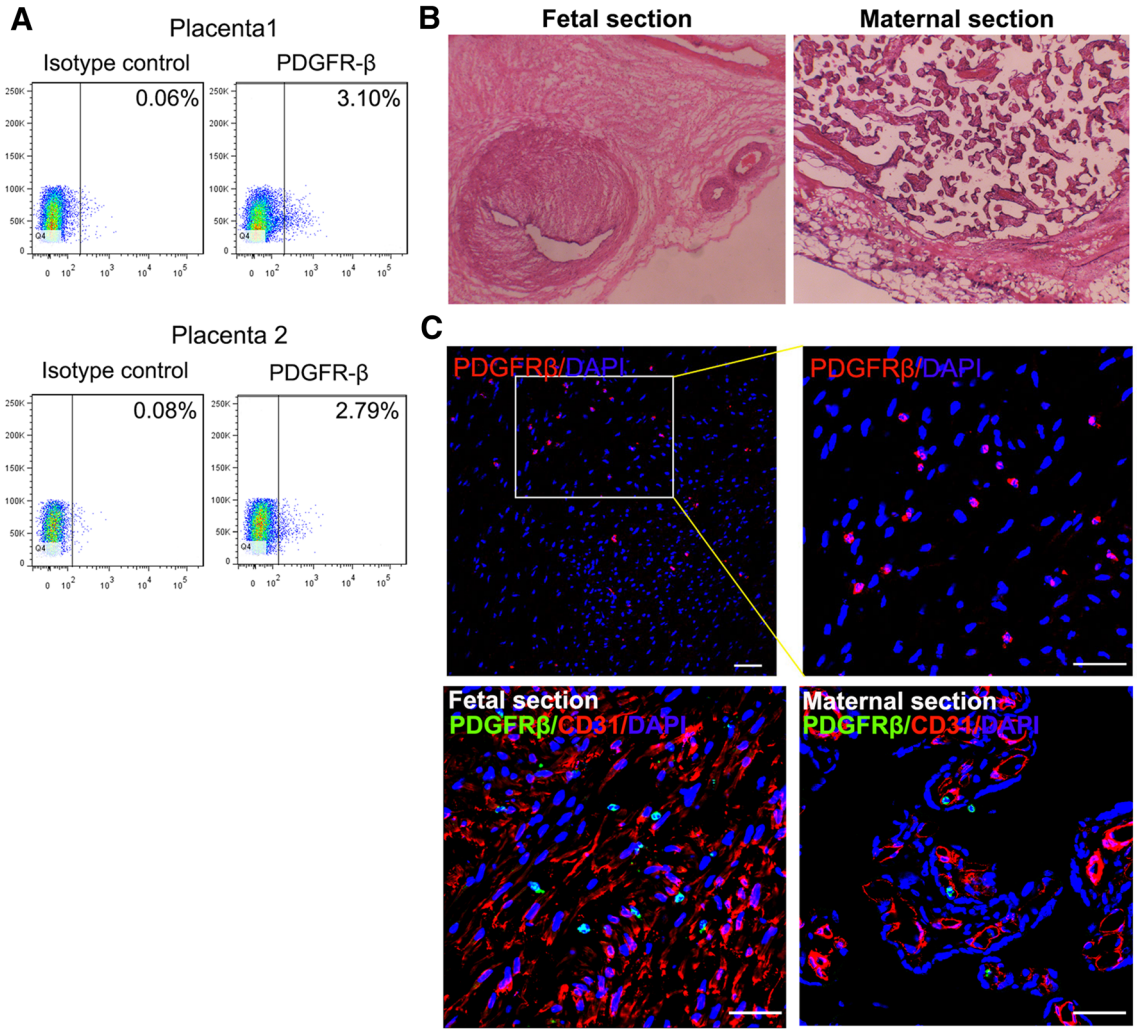

Fig. 1 PDGFR-β$^+$ cells in human placenta. **a** Flow cytometry analysis indicating the fraction of PDGFR-β$^+$ cells in single cell suspensions of fresh placental tissues. **b** Histological images illustrating the structure of fetal and maternal sections of the human placenta (H&E stain). **c** Immunofluorescence staining showed the location of PDGFR-β$^+$ cells (*green*) and their anatomical relevance to blood vessels where endothelial cells were indicated by the expression of CD31 (*red*). Nuclei (*blue*) were stained with DAPI. Samples were analyzed by confocal microscope. *Scale bars* 50 μm

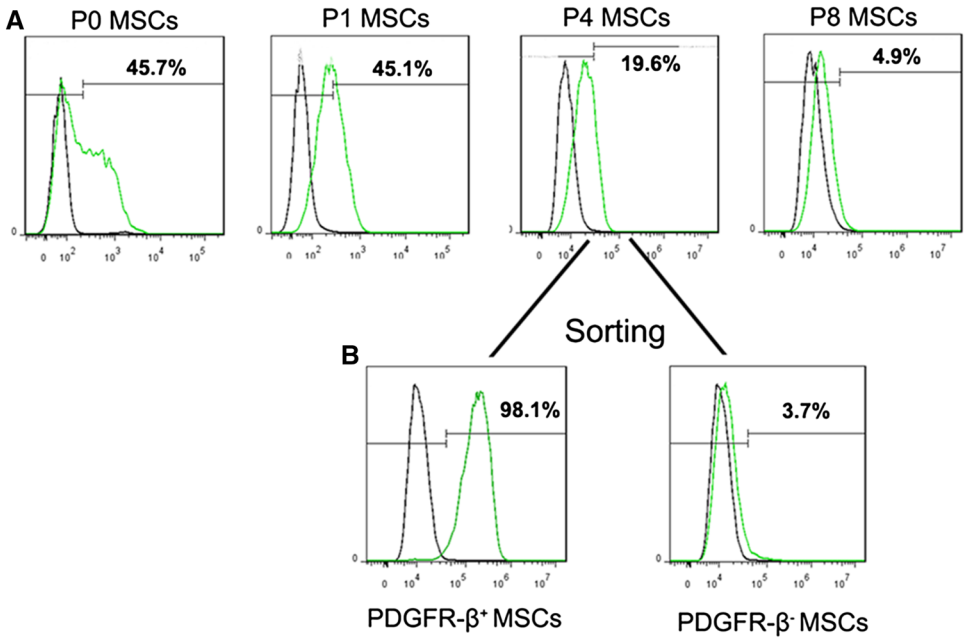

Fig. 2 PDGFR-β expression in human MSCs. **a** Primary PL-MSCs were cultured up to passage 8 and the expression level of PDGFR-β in passages 0, 1, 4 and 8 PL-MSCs were assessed by flow cytometry analysis. PL-MSCs in passage 4 were sorted into PDGFR-β^+ and PDGFR-β^- cells by MACS, and their purities (**b**) and surface expression of certain receptors (**c**, **d**) were determined by flow cytometry

Chemicals were purchased from Sigma-Aldrich except for indication. After 3 weeks of culture with adipogenic induction medium containing 10^{-6} M dexamethasone, 10 µg/ml insulin, and 100 µg/ml 3-isobutyl-L-methylxanthine, cells were stained with oil red O to detect lipids. Osteogenic medium contained 10^{-7} M dexamethasone, 50 µg/ml ascorbic acid, and 10 mM β-glycerophosphate. Cultures at 3 weeks were stained using Alizarin Red for calcium deposition. Chondrogenic differentiation was induced by cultured cells in monolayers or in pellets in a medium containing high-glucose DMEM with 1% penicillin–streptomycin and chondrogenic supplements (1× insulin–transferrin–selenium, 1 µM dexamethasone, 100 µM ascorbic acid-2-phosphate, and 10 ng/ml TGF-β3). After 21 days, pellets were fixed in 4% PFA, sectioned and stained with Alcian blue to assess the presence of glycosaminoglycans and the expression of collagen type II.

Long-term cell engraftment in vivo

Long-term engraftment and adipogenic and osteogenic differentiation of MSCs were performed using a xenograft model [8]. Placental MSCs were sorted into PDGFR-β^+ and PDGFR-β^- cells by MACS. Cells were resuspended in 200 µl of ice-cold phenol red-free Matrigel (BD Bioscience), and subcutaneously injected on the back of 6-week-old male athymic nu/nu mice. To induce osteogenic differentiation, BMP-2 (R&D Systems; https://www.rndsystems.com; 2 µg/implant) was added to the cell–Matrigel mixture prior to implantation. Mice were euthanized and grafts were explanted for histological analysis after 28 days. The presence of adipocytes in the graft was detected after hematoxylin and eosin (H&E) stain, and tissue mineralization was assessed after Von Kossa stain.

Wound healing model and cell transplantation

BABL/C mice and Tie2-GFP transgenic mice were randomly divided into three groups, and excisional wound splinting model was generated as described previously [14, 22]. In brief, after hair removal from the dorsal surface and anesthesia, two 5-mm full-thickness excisional skin wounds were created on each side of the midline. Each wound received 1 million MSCs (PDGFR-β^+ or PDGFR-β^-) which were topically applied onto the wound bed in 20 µl of ice-cold growth factor-reduced Matrigel (BD Biosciences). A silicone splint was placed so that the wound was centered within the splint. Tegaderm (3 M) was placed over the wounds. The animals were housed individually. Digital photographs of wounds were taken at days 0, 3, 7, 10 and 14 and analyzed as previously described [14]. The percentage of wound closure was calculated as follows: (area of original wound − area of actual wound)/area of original wound × 100%.

Histologic examination

Mice were killed at 7 and 14 days, and skin samples including the wound and 4-mm surrounding skin were harvested using a 10-mm biopsy punch. Tissues were fixed overnight in 4% PFA, embedded in paraffin and sectioned (8 µm thick) for H&E stain. For immunofluorescence staining, tissues were embedded in OCT and sectioned (10 µm in thickness). Samples were blocked with 3% BSA in PBS and stained with primary antibodies at appropriate concentrations at

Fig. 2 (continued)

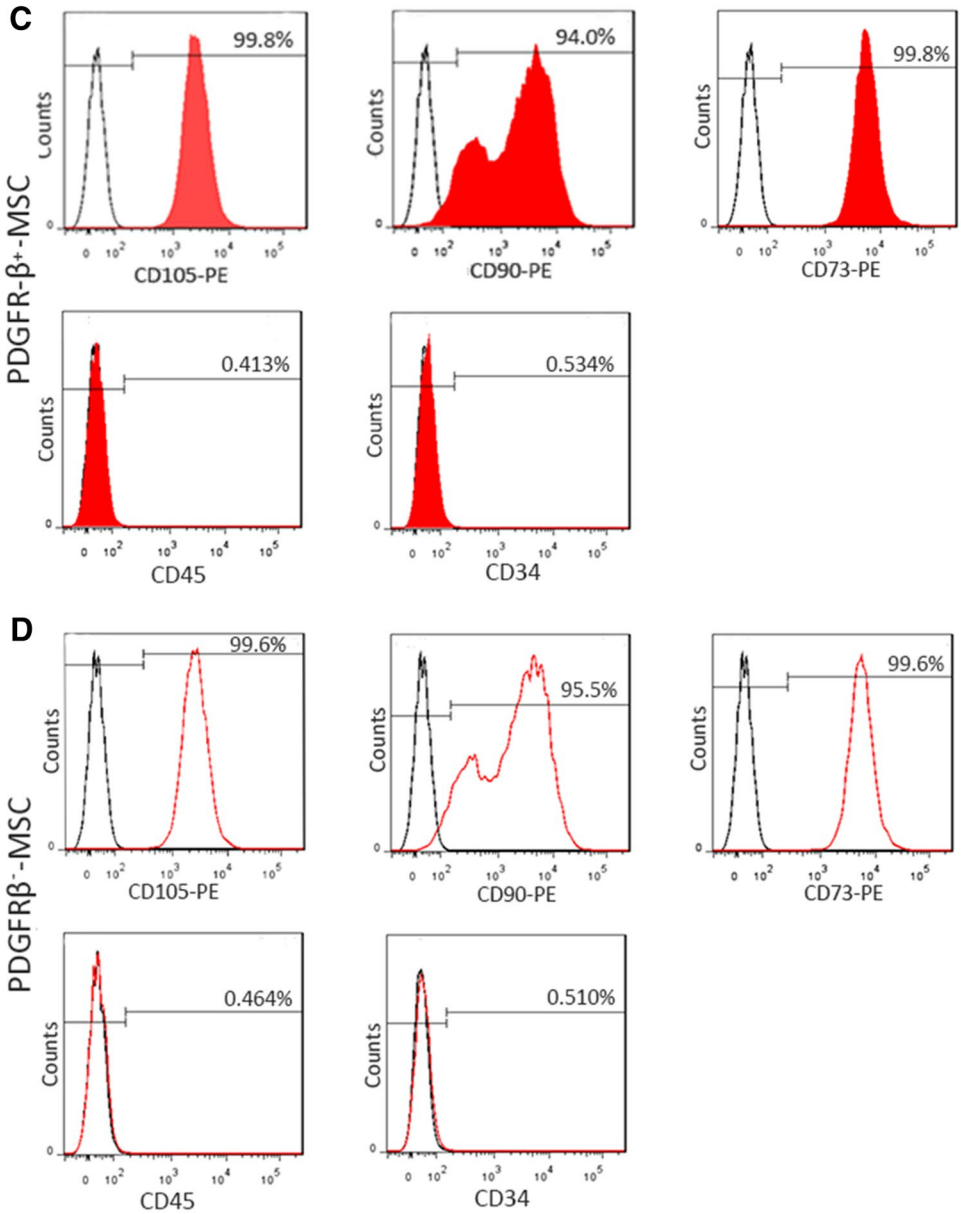

4 °C overnight: anti-mouse CD31 (Abcam, http://www.abcam.cn/), anti-mouse α-SMA (Sigma-Aldrich), anti-biotin PDGFR-β (Miltenyi Biotec), anti-mouse PDGF-B (GeneTex, http://www.genetex.com/). Samples were then stained with FITC-, Cy3-, or tetraethyl rhodamine isothiocyanate (TRITC)-conjugated secondary antibodies (Jackson Immunoresearch, http://www.jacksonimmuno.com). Nuclei were stained with 4′,6-diamidino-2-phenylindole (DAPI). Samples were examined under confocal laser scanning microscope (FV1000, Olympus, http://www.olympus-global.com). To assess neovascular formation after wounding in Tie2-GFP mice, the entire wound and surrounding skin was placed on plastic (tissue culture dish) with the dermis side down and photographed immediately under fluorescence microscope [14].

Real-time PCR analysis

Total RNA was extracted from PDGFR-β^+ or PDGFR-β^- MSCs with TRIzol (Invitrogen) following the manufacturer's instructions. First-strand cDNA was prepared by reverse transcription with Superscript II reverse transcriptase (Invitrogen) and oligo(dT) primers and stored at −20 °C. Real-time polymerase chain reaction (PCR) was performed using SYBR® Premix Ex Taq™ II on an ABI 7300 QPCR System. As an internal control, levels of glyceraldehyde-3-phosphate dehydrogenase (GAPDH) were quantified in parallel with target genes. Normalization and fold changes were calculated using the $\Delta\Delta C_t$ method. Primer sets are indicated in Appendix Table 1.

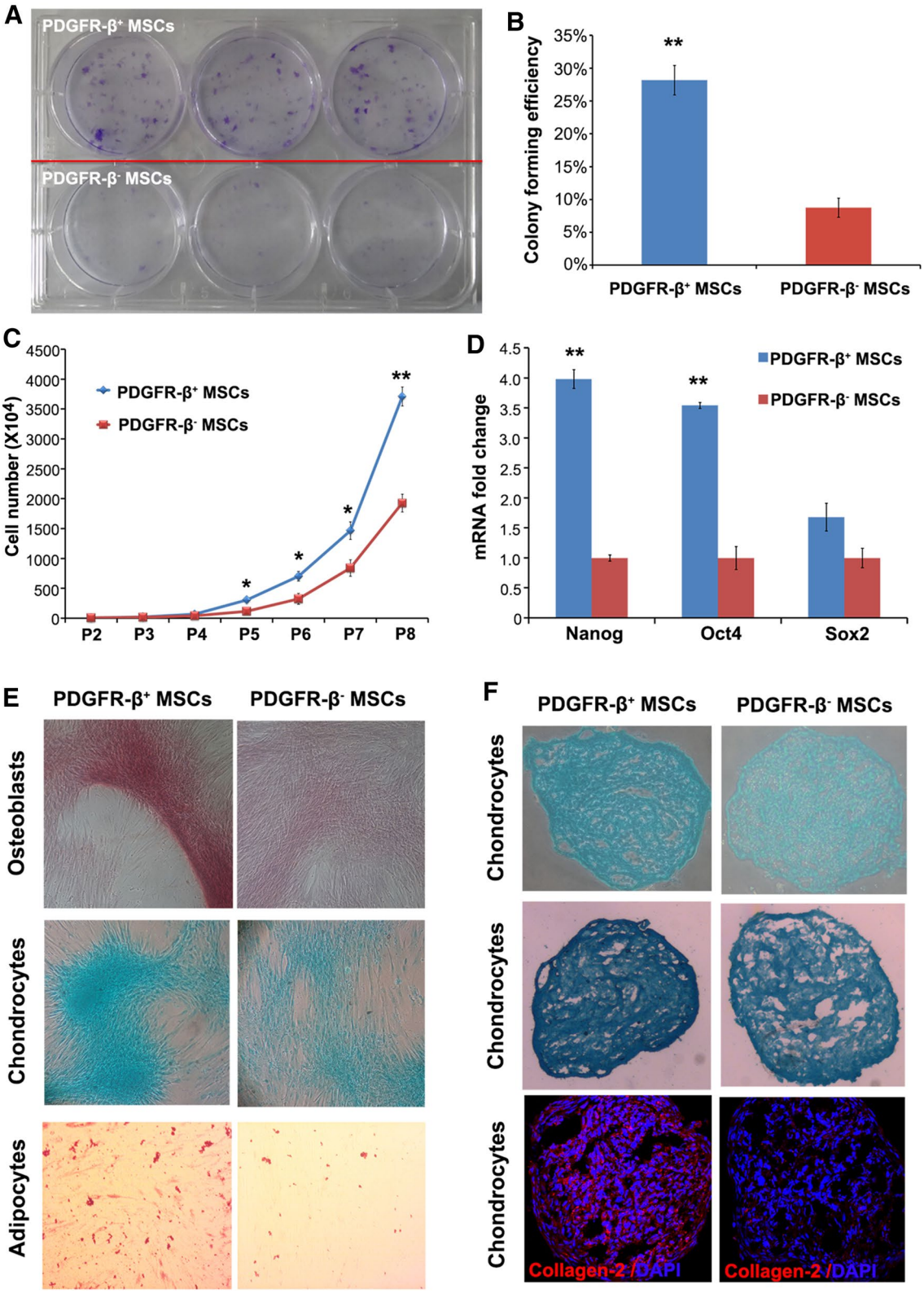
A
PDGFR-β+ MSCs
PDGFR-β- MSCs
B
Colony forming efficiency
35%
30%
25%
20%
15%
10%
5%
0%
**
PDGFR-β+ MSCs
PDGFR-β- MSCs
C
Cell number (X10^4)
4500
4000
3500
3000
2500
2000
1500
1000
500
0
PDGFR-β+ MSCs
PDGFR-β- MSCs
**
*
*
*
P2
P3
P4
P5
P6
P7
P8
D
mRNA fold change
4.5
4.0
3.5
3.0
2.5
2.0
1.5
1.0
0.5
0
**
**
PDGFR-β+ MSCs
PDGFR-β- MSCs
Nanog
Oct4
Sox2
E
PDGFR-β+ MSCs
PDGFR-β- MSCs
Osteoblasts
Chondrocytes
Adipocytes
F
PDGFR-β+ MSCs
PDGFR-β- MSCs
Chondrocytes
Chondrocytes
Chondrocytes
Collagen-2 /DAPI
Collagen-2 /DAPI

◀**Fig. 3** Multipotency of PDGFR-β$^+$ MSCs. **a**, **b** PDGFR-β$^+$ cells and PDGFR-β$^-$ cells were seeded, respectively, in six-well culture plate at a density of 200 cells per well and incubated for 14 days. Then the culture was fixed with 4% PFA and stained with crystal violet solution. Triplet wells were used for the assay (**a**). The number of colonies (diameter ≥2 mm) in each well was counted (**b**). **c** Growth curves of PDGFR-β$^+$ cells and PDGFR-β$^-$ MSCs. **d** Real-time PCR analysis of the expression of Nanog, Oct4 and Sox2 in PDGFR-β$^+$ and PDGFR-β$^-$ MSCs. **e** Differentiation of MSC. PDGFR-β$^+$ MSCs and PDGFR-β$^-$ MSCs were examined for their differentiation into osteoblasts, chondrocytes and adipocytes in monolayer culture upon appropriate inductions. For osteogenic differentiation the culture was examined after Alizarin Red S stain; for chondrogenesis the culture was assessed after Alcian blue stain; for adipogenic differentiation the cells were analyzed after oil red stain. **f** Chondrogenesis in pellet culture was determined for their expression of proteoglycans after Alcian blue stain and their expression of collagen II after immunofluorescence stain. **g**, **h** In in vivo differentiation analysis, equal numbers of PDGFR-β$^+$ or PDGFR-β$^-$ MSCs in Matrigel were implanted subcutaneously in nude mice (for osteogenesis BMP-2 was added to the implants, 2 μg/implant). After 28 days, the grafts were removed for histological analysis. In assessing osteogenesis, tissue sections were stained by Von Kossa and H&E (**g**, $n = 4$); adipogenesis in the grafts were determined for the presence of cells with adipocyte morphology after H&E stain (**f**, $n = 4$). $^{***}P < 0.001$, $^{**}P < 0.01$, $^{*}P < 0.05$

Chemotaxis assay

Chemotaxis assay of PDGFR-β$^+$ and PDGFR-β$^-$ MSCs was performed in 24-well plates containing 8-μm porosity inserts (Corning, http://www.corning.com/). The cells were washed twice with serum-free DMEM and suspended as 5×10^5/ml in DMEM containing 0.5% BSA. Cells (2.5×10^4) in 50 μl were loaded onto the top well. Serum-free DMEM containing 10 ng/ml PDGF-BB, or fresh extracts of day-2 wound tissues were added to the bottom chamber with a total volume of 0.6 ml. In some experiments, PDGFR-β$^+$ MSCs were pre-treated with a functional blocking antibody against PDGFR-β (R&D Systems, UK) at 30 μg/ml. After 4 h of incubation, the non-migrating cells were completely wiped from the top surface of the filters, and the migrating cells adhering to the undersurface of the filters were stained with DAPI and quantified with an imaging software (Image J).

Enzyme-linked immunosorbent assay (ELISA)

Equal numbers of PDGFR-β$^+$ or PDGFR-β$^-$ MSCs were seeded in six-well tissue culture dishes in DMEM and incubated for 24 h. Media were collected, centrifuged and stored at −80 °C. Human fibroblast growth factor basic (bFGF), vascular endothelial growth factor (VEGF)-a, interleukin (IL)-10 and IL-4 in the media were measured using ELISA kits (R&D system) following the manufacturer's instructions.

Statistical analysis

All data were expressed as mean ± SD. Data were compared using unpaired Student's *t* tests. Comparisons between multiple groups were performed by ANOVA. $P < 0.05$ was considered statistically significant.

Results

PDGFR-β$^+$ cells in human placenta

To determine the abundant PDGFR-β$^+$ cells in human placenta, fresh placental tissues were enzymatically dispersed to form single cell suspensions. Analysis of the single cell suspensions by flow cytometry indicated that approximately 2.94 ± 0.21% of total placental cells expressed PDGFR-β ($n = 4$; Fig. 1a). To determine the location of PDGFR-β$^+$ cells in the placenta, we dissected the placenta horizontally into three equal sections, the fetal side section, the middle section and the maternal side section. Histological analysis showed that the fetal side section was largely composed of blood vessels and connective tissues, while the material side section mainly consisted of villi (Fig. 1b). Immunofluorescence analysis of the placental tissue revealed that PDGFR-β$^+$ cells were present in clusters with relatively higher incidences in the fatal side section and were in close adjacency to blood vessels (Fig. 1c).

PDGFR-β$^+$ MSCs exhibit increased multipotency

Placental cell suspensions were seeded on tissue culture plates in MSC growth medium. After 24 h, the majority of the cells which remained in suspension were removed by changing medium. Cell colonies appeared after approximately 7 days. When reaching 80 confluence, colonies were harvested and pooled. Flow cytometry analysis showed that the cells were negative for lineage cell markers such as CD34 and CD45, and over 95% of the cells were strongly positive for CD105, CD73 and CD90, exhibiting typical immunophenotypic features of MSCs [18]. Notably, approximately 45% of the cells in early passages expressed PDGFR-β on the surface, and with successive culture the proportion of PDGFR-β-expressing MSCs decreased to approximately 20% in passage 4 (Fig. 2a), suggesting that the surface expression of the receptor was unstable in current culture system, like many other receptors [3, 23].

We sorted MSCs in passage 4 into PDGFR-β$^+$ and PDGFR-β$^-$ subpopulations (Fig. 2b). Immunophenotypic analysis of the cells revealed that the two cell subsets expressed similar levels of CD105, CD90 and CD73, and did not express CD45 and CD34 (Fig. 2c, d). We next examined whether PDGFR-β$^+$ MSCs differed from PDGFR-β$^-$ MSCs

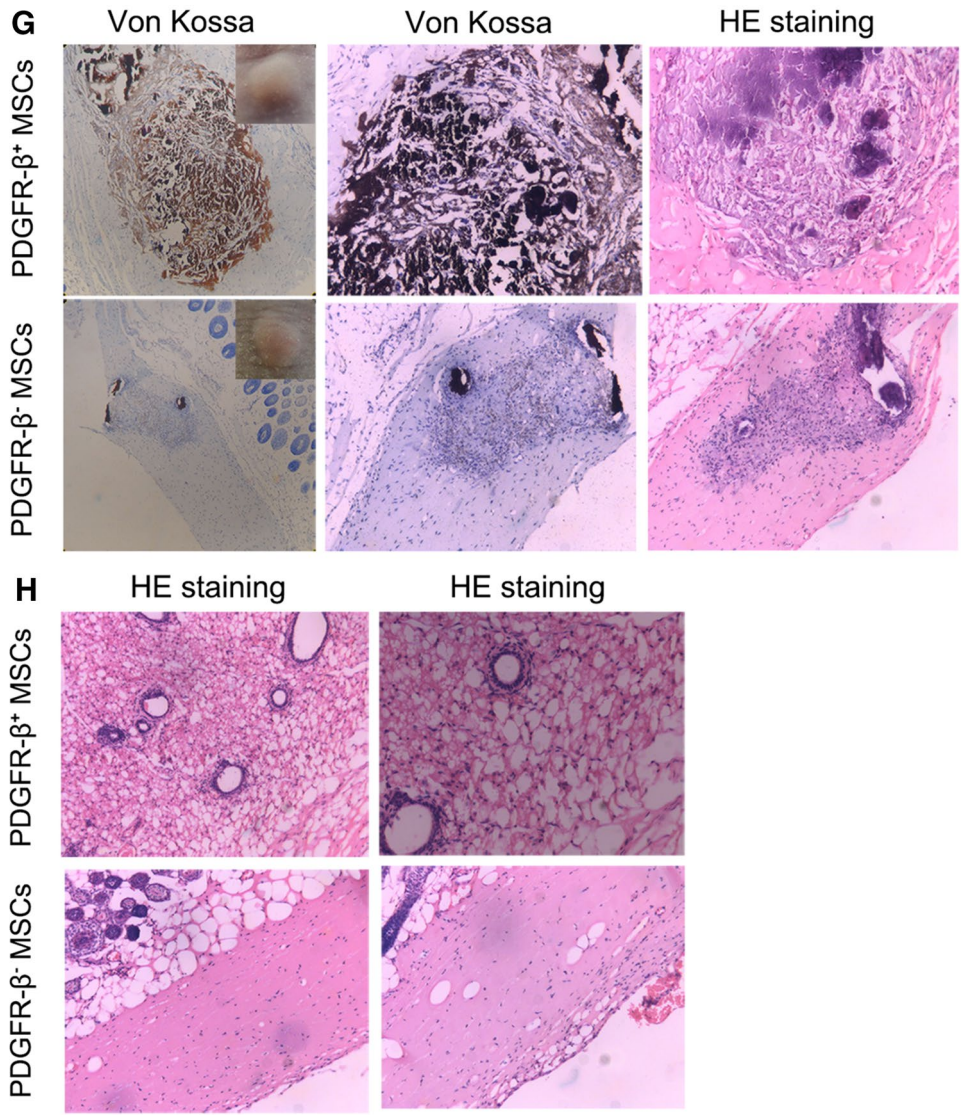

Fig. 3 (continued)

in differentiation potency. When equal number of PDGFR-β^+ MSCs and PDGFR-β^- MSCs were seeded in low density, PDGFR-β^+ MSCs formed significantly more colonies (CFU-F) than PDGFR-β^- MSCs (Fig. 3a, b). Consistently, PDGFR-β^+ MSCs grew faster and showed higher expression levels of pluripotent genes Nanog, Oct4 and Sox2, compared to PDGFR-β^- MSCs, as determined by real-time PCR analysis (Fig. 3c, d).

In vitro differentiation analysis indicated that PDGFR-β^+ MSCs exhibited enhanced osteogenic, chondrogenic and adipogenic differentiation upon incubation with corresponding induction media, compared to PDGFR-β^- MSCs (Fig. 3e). After osteogenic induction, PDGFR-β^+ MSCs showed more abundant calcium deposition than PDGFR-β^- MSCs, as determined after Alizarin red staining. Similarly, upon chondrogenic induction, PDGFR-β^+ MSCs exhibited higher glycosaminoglycan production as determined by Alcian blue stain (Fig. 3e). Consistently, in spheroid culture, PDGFR-β^+ MSCs showed higher levels of collagen II expression than PDGFR-β^- MSCs as determined by immunofluorescence analysis (Fig. 3f). In addition, more PDGFR-β^+ MSCs differentiated into oil red O-positive adipocytes than PDGFR-β^- MSCs upon induction (Fig. 3e).

We further examined whether PDGFR-β^+ MSCs had enhanced osteogenic and adipogenic differentiation ability in vivo. To assess osteogenic differentiation, 10^6 PDGFR-β^+ MSCs or PDGFR-β^- MSCs in Matrigel were implanted subcutaneously in nude mice in the presence of 2 μg/implant BMP-2. 28 days later, grafts were removed for histological analysis. Von Kossa stain showed that PDGFR-β^+ MSC grafts had evidently larger areas of mineralization compared to PDGFR-β^- MSC grafts (Fig. 3g). To determine

adipogenic differentiation, subcutaneous implants of 10^6 PDGFR-β^+ MSCs or PDGFR-β^- MSCs in nude mice were examined at day 28 for the presence of adipocytes; the results showed much more adipocytes in the PDGFR-β^+ MSC grafts (Fig. 3h).

PDGFR-β^+ MSCs express higher levels of pro-angiogenic cytokines

We examined whether PDGFR-β^+ MSCs were better involved in angiogenesis. Real-time PCR analysis indicated that PDGFR-β^+ MSCs expressed higher levels of pro-angiogenic genes such as *VEGFA* (encoding VEGF-a), *FGF2* (encoding bFGF), *PDGFA* (encoding PDGF-A) and *PDGFB* (encoding PDGF-B), compared to PDGFR-β^- MSCs (Fig. 4a). Moreover, ELISA analysis of MSC-conditioned media indicated that PDGFR-β^+ MSCs secreted greater amounts of bFGF (Fig. 4b), VEGF-a (Fig. 4c) and IL-10 (Fig. 4e), and similar amounts of IL-4, compared to PDGFR-β^- MSCs (Fig. 4d).

PDGFR-β^+ MSCs promote angiogenesis

We next examined if PDGFR-β^+ MSCs exerted an enhanced effect on angiogenesis. One million PDGFR-β^+ or PDGFR-β^- MSCs in Matrigel were applied to excisional wounds in Tie2-GFP transgenic mice; wounds treated with Matrigel alone (Sham) were used as a control. Fluorescence microscopic analysis of the whole skin-mounted wounds at day 7 showed that in PDGFR-β^+ MSC-treated wounds fine blood vessels extended into the wound bed from the surrounding tissues, while much fewer vessels were detected in PDGFR-β^- MSC-treated wounds or in Sham wounds (Fig. 5a).

To track MSCs in wounds, GPF-labeled MSCs were implanted into wounds in BABL/C mice. Immunofluorescence analysis of day-7 wounds showed that GFP$^+$/PDGFR-β^+ MSCs migrated down into the wound bed tissue, while GFP$^+$/PDGFR-β^- MSCs largely remained in the top layer of the wound bed tissue (Fig. 5b). Immunostaining for α-smooth actin (α-SMA) or endothelial protein CD31 in day-7 and day-14 wound tissues demonstrated that the vasculature density was markedly higher in PDGFR-β^+ MSC-treated wounds, compared to PDGFR-β^-MSC-treated wounds or Sham wounds (Fig. 5b, c). Notably, GFP-labeled PDGFR-β^+ MSCs were in close association with the new vasculature in the wound tissue (Fig. 5d). Some of the PDGFR-β^+ MSCs in the vasculature expressed α-SMA (Fig. 5d).

PDGFR-β^+ MSCs accelerate wound healing

To examine whether PDGFR-β^+ MSCs were superior to PDGFR-β^- MSCs in wound healing, one million PDGFR-β^+ or PDGFR-β^- MSCs in Matrigel were transplanted into excisional wounds in BALB/C mice; Sham control wounds were treated with Matrigel alone. Wound sizes were monitored at days 3, 7, 10 and 14, and the result indicated that PDGFR-β^+ MSCs were superior to PDGFR-β^- MSCs in accelerating wound closure at all time points (Fig. 6a, b). Histological analysis of day-7 wounds indicated that the re-epithelialization in PDGFR-β^+ MSC-treated wounds was enhanced compared to PDGFR-β^- MSC-treated wounds or Sham wounds. In addition, PDGFR-β^+ MSC-treated wounds exhibited increased cellularity and thicker granulation tissues at day 7 and day 14, compared to PDGFR-β^- MSC-treated wounds or Sham wounds (Fig. 6c). To determine MSC engraftment, the percentages of GFP$^+$ MSCs in wound single cell suspensions were analyzed by flow cytometry, and the number of MSCs per wound was calculated. At day 7, the average number of MSCs per wound was $3.92 \pm 0.31 \times 10^5$ in PDGFR-β^+ MSC-treated wounds ($n = 3$), and $2.46 \pm 0.26 \times 10^5$ in PDGFR-β^- MSC-treated wounds ($n = 3$) (Fig. 6d, e, $P < 0.05$). Taking the initially implanted 1 million MSCs per wound as 100%, after calculation, the engraftment rates were 39.2 and 24.6% for PDGFR-β^+ MSCs and PDGFR-β^- MSCs, respectively ($P < 0.05$).

PDGFR-β^+ MSCs exhibit enhanced chemotactic migration

We observed that GFP$^+$ PDGFR-β^+ MSCs were present deep into the wound bed tissue at day 7, while GFP$^+$ PDGFR-β^- MSCs remained on the surface of the wound bed after topical application (Fig. 5b, d). This phenomenon suggests that PDGFR-β^+ MSCs might have enhanced chemotactic migration to certain chemoattractants in the wound tissue. To test this hypothesis, we examined the migration of MSCs to PDGF-BB, the ligand of PDGF-β. Transwell migration analysis indicated that the number of PDGFR-β^+ MSCs migrated toward PDGF-BB was eightfold more, and the number of PDGFR-β^+ MSCs migrated in response to fresh day-2 wound tissue extracts was threefold higher, than PDGFR-β^- MSCs (Fig. 7a, b). Pre-treatment of PDGFR-β^+ MSCs with a functional blocking antibody against PDGFR-β significantly reduced their migration toward PDGF-BB or the fresh wound tissue extracts ($P < 0.01$). We then examined the expression of PDGF-B in the skin after wounding. Real-time PCR analysis showed that the expression level of *PDGFB* was upregulated after wounding, which peaked at day 2 (fivefold increase), and returned to basal level at day 7 (Fig. 7c). In consistence, immunofluorescence analysis showed that the level of PDGF-B in the wound tissue was markedly higher than that in the unwounded skin tissue (Fig. 7d). Taken together, these results suggest that PDGFR-β plays a crucial role in chemotactic migration and engraftment of MSCs into the wound.

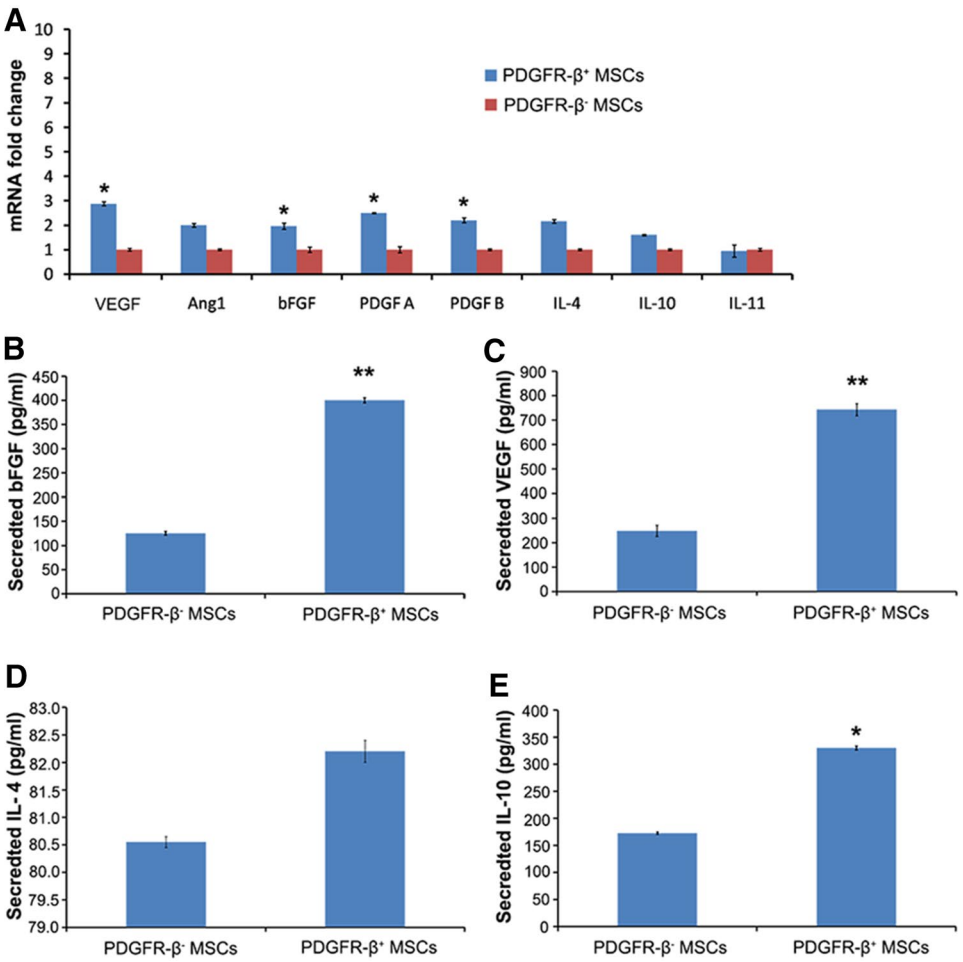

Fig. 4 Expression of endothelial genes and angiogenic cytokines. **a** Real-time PCR analysis of the expression of CD31, VE-cadherin, VEGF-a, Ang1, bFGF, PDGF-A, PDGF-B, IL-4, IL-10 and IL-4 in PDGFR-β^+ MSCs and PDGFR-β^- MSCs. ELISA assay determining the levels of bFGF (**b**), VEGF-a (**c**), IL-4 (**d**) and IL-10 (**e**) in PDGFR-β^+ MSC- or PDGFR-β^- MSC-conditioned medium ($n = 3$, $^{***}P < 0.001$, $^{**}P < 0.01$, $^{*}P < 0.05$)

Discussion

Mesenchymal stem cells are defined as multipotent stem cells. However, previous studies suggest that MSC culture contains cells with different differentiation potencies, from unipotent to multipotent [3, 24]. In this study, we found that PDGFR-β^+ MSCs exhibited enhanced differentiation potential towards osteogenesis, chondrogenesis and adipogenesis, indicating superior multipotency over PDGFR-β^- MSCs. In consistence, PDGFR-β^+ MSCs showed enhanced growth rate and clonogenesis. Our results are in line with two recent studies where PDGF-AB in combination with 5-azacytidine (AZA) converted osteoblasts into multipotent stem cells with multi-germ layer differentiation potential [25], and PDGF-A was involved with the reprogramming of fibroblasts into cardiovascular progenitor cells [26]. These data suggest that PDGF signaling is involved in the gain and maintenance of stem cell potency. Meanwhile, a previous study showed that pharmaceutical inhibition of PDGFR (which suppressed the phosphorylation of both PDGFR-α and PDGFR-β) in human bone marrow-derived MSCs upregulated the expression of pluripotent factors Oct4A and Nanog [27], implying that a simultaneous suppression of the two receptors may lead to different outcomes.

The pro-angiogenic effect of MSCs has been reported in several previous studies [14, 28, 29]. Recently, a study showed that VCAM-1^+ MSCs derived from placental chorionic villi, which accounted for 68% of MSCs in culture, exhibited enhanced effect in angiogenesis [29]. Interestingly, a previous study showed that the proliferation potential and CFU-F-generating capacity of bone marrow-derived MSCs were negatively associated with donor ages in humans, while the level of VCAM-1 in MSCs increased with donor ages, which was likely due to increased inflammation levels in the elderly as the expression of VCAM-1 could be upregulated by proinflammatory cytokines [30]. In the present study, we

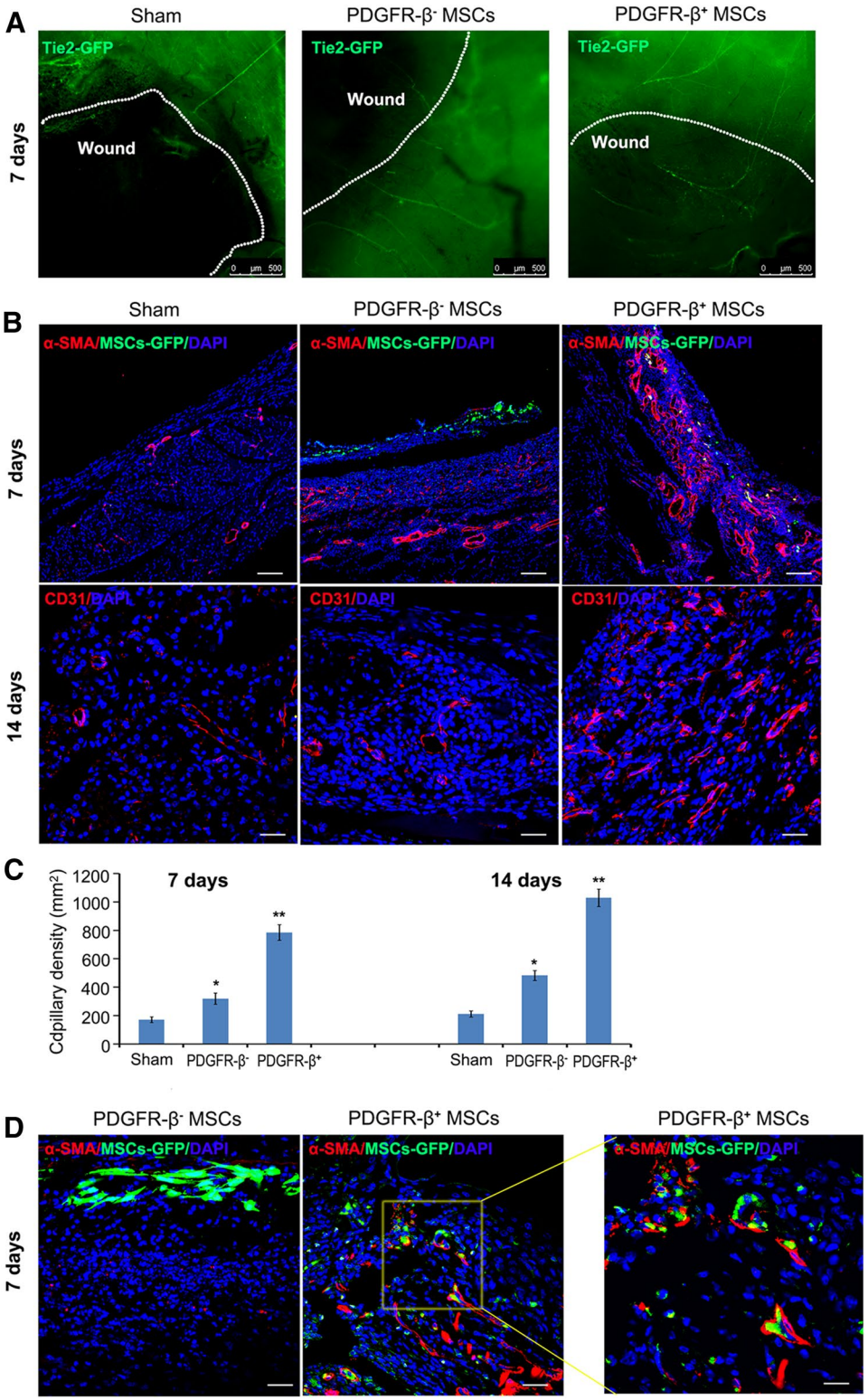

Fig. 5 PDGFR-β$^+$ MSCs in neovascularization. **a** Wounds were generated in *Tie2*-transgenic mice and treated with vehicle medium (Sham), PDGFR-β$^-$ MSCs, or PDGFR-β$^+$ MSCs. Fluorescence microscopic examination of whole skin-mounted wounds at day 7 showed new vasculature in the wound, which was more evident in PDGFR-β$^+$ MSC-treated wounds. **b–d** Immunofluorescence analysis of the wound tissue sections at day 7 (*upper panel*, *scale bars* 60 μm) and day 14 (*lower panel*, *scale bars* 30 μm) in wild-type BALB/C mice whose wounds received topical application of GFP-labeled MSCs (*green*) or vehicle medium (Sham). To detect vasculature, sections were stained with anti-α-SMA antibody (day-7 wounds, *red*) or anti-CD31 antibody (day-14 wounds, *red*) (**b**). Capillary densities in the day-7 and day-14 wounds were assessed (**c**, $n = 6$; $^{**}P < 0.01$, $^{*}P < 0.05$). In the day-7 wounds, GFP-labeled PDGFR-β$^-$ MSCs (*green*) remained on the top of the wound bed, while GFP-labeled (*green*) PDGFR-β$^+$ MSCs migrated into the wound tissue (**b**) and formed close association with α-SMA$^+$ cells in the neovasculature; some of them co-expressed α-SMA (**d**). Nuclei were stained with DAPI. *Scale bars* 30 μm

found that PDGFR-β, a receptor highly expressed in perivascular MSCs [5, 31], identified a subset of placental MSCs with substantially superior effect in promoting neovascularization in the wound. In addition, the expression level of PDGFR-β decreased progressively in adherent culture upon passaging, indicating that the expression of the receptor in current culture regime is unstable. Similarly, several other receptors have been found with declining expression in MSCS upon successive passages such as CXCR4, CCR1 and CCR7 [3, 23, 32]. In accordance, MSCs exhibited decreased

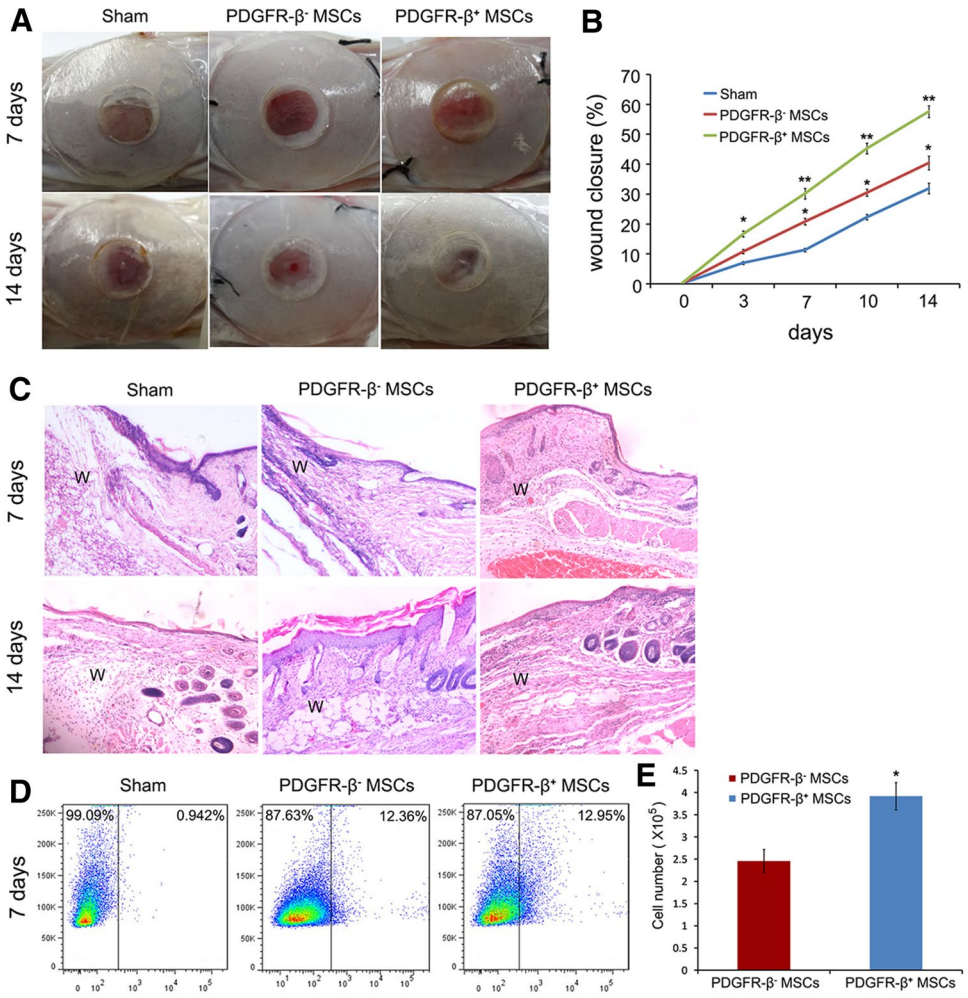

Fig. 6 PDGFR-β$^+$ MSCs in wound healing. **a**, **b** Excisional wounds in BALB/C mice received topical application of one million PDGFR-β$^-$ MSCs, PDGFR-β$^+$ MSCs, or vehicle medium (Sham). Representative images of the wounds at days 7 and 14 were shown (with transparent Tegaderm dressing) (**a**). Quantitative evaluation of wound closure rates in Sham wounds ($n = 9$), PDGFR-β$^-$ MSC-treated wounds ($n = 12$), and PDGFR-β$^+$ MSC-treated wounds ($n = 12$) (**b**). PDGFR-β$^+$ MSCs versus Sham or PDGFR-β$^-$ MSCs, $^{**}P < 0.01$, $^{*}P < 0.05$. **c** Histological analysis of wounds at days 7 and 14 (H&E stain) showed increased cellularity in PDGFR-β$^+$ MSC-treated wounds. *W* wound. **d**, **e** The number of cells per day-7 wound was assessed by counting the cells in the single cell suspension of the wound, and the percentage of GFP$^+$ cells in the single cell suspension was determined by flow cytometry (**d**), cells from Sham wounds were used as negative controls and for gate setting. The number of cells per wound was calculated (**e**, $n = 4$, $^{*}P < 0.05$)

differentiation potency and therapeutic efficacy after culture expansion [18, 33–35].

Our results indicate that PDGFR-β is necessary for MSCs migration and engraftment into the wound. Previous studies indicated that PDGFs bound to PDGFRs on the surface of MSCs, and PDGFR-β was the major receptor for PDGF-AA- and PDGF-BB-induced MSC migration [36, 37]. A recent study showed that co-transplantation of endothelial colony-forming cells enhanced the survival and engraftment of bone marrow-derived MSCs largely through secretion of PDGF-BB [8]. In consistence with these findings, we showed that PDGFR-β$^+$ MSCs migrated toward PDGF-BB or wound tissue extracts was several fold more than PDGFR-β$^-$ MSCs, and MSCs lacking PDGFR-β failed to migrate into the wound tissue after topical application, resulting in reduced engraftment, angiogenesis and wound healing effect. PDGF-B was upregulated after wounding to the skin. These data suggests that PDGFR-β is important for the recruitment of MSCs to the site of tissue injury where neovascularization occurs.

Previous studies indicate that MSCs promote angiogenesis largely through secretion of pro-angiogenic factors [14, 17, 38, 39]. In agreement with these findings, we found that PDGFR-β$^+$ MSCs expressed higher levels of cytokines known to promote angiogenesis such as VEGF-a, bFGF and IL-10 in association with enhanced angiogenesis. In addition, we showed that PDGFR-β$^+$ MSCs migrated into the wound and contributed to α-SMA-expressing smooth muscle cells in the neovasculature. Our data are in line with observations, where MSCs were induced to differentiate into cells with smooth muscle cell properties in vitro [40, 41]. Taken together, our results suggest that PDGFR-β$^+$ MSCs enhance angiogenesis through releasing pro-angiogenic factors and direct contribution to vascular wall cells.

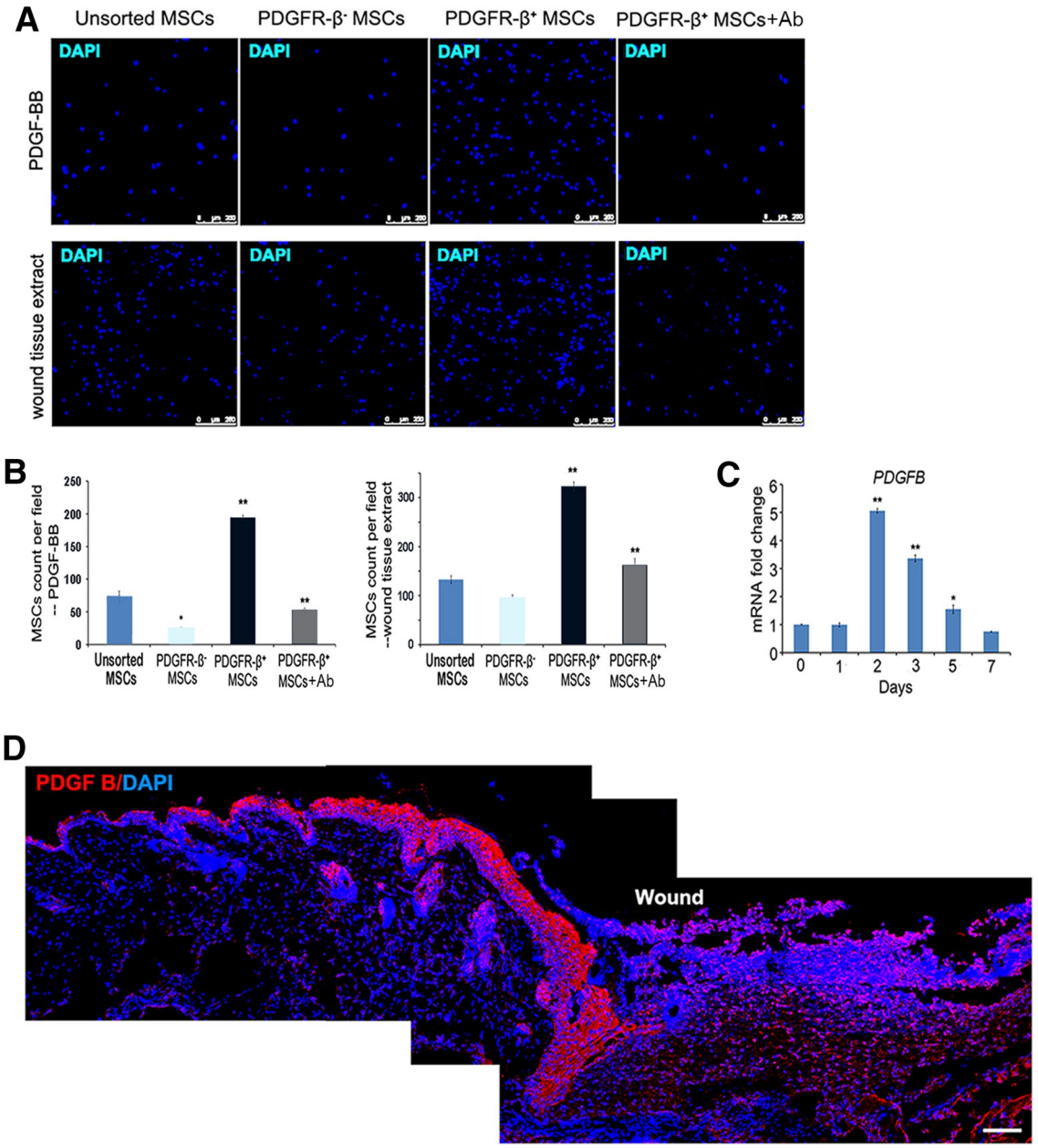

Fig. 7 Chemotactic migration of PDGFR-β^+ MSCs. **a**, **b** Transwell migration assay showed that the migration of unsorted MSCs, PDGFR-β^+ MSCs and PDGFR-β^- MSCs in response to PDGF-BB or fresh wound tissue extracts. Nuclei were stained with DAPI (**a**). The average number of cells migrated across the pores per microscopic field was quantified by Image J (**b**). Pre-treatment of PDGFR-β^+ MSCs with a functional blocking antibody against PDGFR-β significantly reduced their migration toward PDGF-BB or the fresh wound tissue extracts (**a**, **b**). Experiments were performed in triplicate wells. **c**, **d** Real-time PCR analysis of the expression of *PDGFB* after wounding in mice (**c**). **d** Immunofluorescence analysis of a day-3 wound showed the expression of PDGF-B (*red*), which showed higher levels in the wound bed tissue and the tissue adjacent to the wound. Nuclei were stained with DAPI. *Scale bars* 50 μm. $^{***}P < 0.001$, $^{**}P < 0.01$, $^{*}P < 0.05$

Conclusions

Our study demonstrated that the PDGFR-β^+ MSC subpopulation displayed a superior angiogenic property and exerted enhanced therapeutic efficacy on cutaneous wound healing in comparison with the PDGFR-β^- MSC subpopulation. The study may provide a novel strategy to achieve enhanced effect for MSC-based therapies for ischemic diseases.

Acknowledgements We gratefully thank Bing Yu for assistance in confocal analysis. This work was supported by grants from

Natural Science Foundation of China (Nos. 31371404, 31571429), Natural Science Foundation of Guangdong (2015A030311041), and Shenzhen Science and Technology Innovation Committee (JCY20160301150838144).

Author contributions SW: performed experiments and data analysis; SS, MM, JW, BS: performed experiments; LY: provided materials and designed experiments; XF, ET: designed experiments; YW: designed experiments and wrote the manuscript.

Compliance with ethical standards

Conflict of interest The authors report no conflicts of interest.

References

1. Trounson A, McDonald C (2015) Stem cell therapies in clinical trials: progress and challenges. Cell Stem Cell 17(1):11–22. doi:10.1016/j.stem.2015.06.007
2. Parekkadan B, Milwid JM (2010) Mesenchymal stem cells as therapeutics. Annu Rev Biomed Eng 12:87–117. doi:10.1146/annurev-bioeng-070909-105309
3. Mo M, Wang S, Zhou Y et al (2016) Mesenchymal stem cell subpopulations: phenotype, property and therapeutic potential. Cell Mol Life Sci 73(17):3311–3321. doi:10.1007/s00018-016-2229-7
4. Phinney DG (2012) Functional heterogeneity of mesenchymal stem cells: implications for cell therapy. J Cell Biochem 113(9):2806–2812. doi:10.1002/jcb.24166
5. Hellstrom M, Kalen M, Lindahl P et al (1999) Role of PDGF-B and PDGFR-beta in recruitment of vascular smooth muscle cells and pericytes during embryonic blood vessel formation in the mouse. Development 126(14):3047–3055
6. Rajkumar VS, Shiwen X, Bostrom M et al (2006) Platelet-derived growth factor-beta receptor activation is essential for fibroblast and pericyte recruitment during cutaneous wound healing. Am J Pathol 169(6):2254–2265
7. Tokunaga A, Oya T, Ishii Y et al (2008) PDGF receptor beta is a potent regulator of mesenchymal stromal cell function. J Bone Miner Res 23(9):1519–1528. doi:10.1359/Jbmr.080409
8. Lin RZ, Moreno-Luna R, Li D et al (2014) Human endothelial colony-forming cells serve as trophic mediators for mesenchymal stem cell engraftment via paracrine signaling. Proc Natl Acad Sci USA 111(28):10137–10142. doi:10.1073/pnas.1405388111
9. Falanga V (2005) Wound healing and its impairment in the diabetic foot. Lancet 366(9498):1736–1743. doi:10.1016/S0140-6736(05)67700-8
10. Singer AJ, Clark RA (1999) Cutaneous wound healing. N Engl J Med 341(10):738–746. doi:10.1056/NEJM199909023411006
11. Cha J, Falanga V (2007) Stem cells in cutaneous wound healing. Clin Dermatol 25(1):73–78. doi:10.1016/j.clindermatol.2006.10.002
12. Otero-Vinas M, Falanga V (2016) Mesenchymal stem cells in chronic wounds: the spectrum from basic to advanced therapy. Adv Wound Care 5(4):149–163. doi:10.1089/wound.2015.0627
13. DiPietro LA (2016) Angiogenesis and wound repair: when enough is enough. J Leukoc Biol 100(5):979–984. doi:10.1189/jlb.4MR0316-102R
14. Wu Y, Chen L, Scott PG et al (2007) Mesenchymal stem cells enhance wound healing through differentiation and angiogenesis. Stem Cells 25(10):2648–2659. doi:10.1634/stemcells.2007-0226
15. Wu Y, Zhao RC, Tredget EE (2010) Concise review: bone marrow-derived stem/progenitor cells in cutaneous repair and regeneration. Stem Cells 28(5):905–915. doi:10.1002/stem.420
16. Li M, Zhao Y, Hao H et al (2015) Mesenchymal stem cell-based therapy for nonhealing wounds: today and tomorrow. Wound Repair Regeneration 23(4):465–482. doi:10.1111/wrr.12304
17. Chen L, Tredget EE, Wu PY et al (2008) Paracrine factors of mesenchymal stem cells recruit macrophages and endothelial lineage cells and enhance wound healing. PLoS One 3(4):e1886. doi:10.1371/journal.pone.0001886
18. Li Z, Liu C, Xie Z et al (2011) Epigenetic dysregulation in mesenchymal stem cell aging and spontaneous differentiation. PLoS One 6(6):e20526. doi:10.1371/journal.pone.0020526
19. Wang S, Guo L, Ge J et al (2015) Excess integrins cause lung entrapment of mesenchymal stem cells. Stem Cells 33(11):3315–3326. doi:10.1002/stem.2087
20. Guo L, Zhou Y, Wang S et al (2014) Epigenetic changes of mesenchymal stem cells in three-dimensional (3D) spheroids. J Cell Mol Med 18(10):2009–2019. doi:10.1111/jcmm.12336
21. Pittenger MF, Mackay AM, Beck SC et al (1999) Multilineage potential of adult human mesenchymal stem cells. Science 284(5411):143–147
22. Wang X, Ge J, Tredget EE et al (2013) The mouse excisional wound splinting model, including applications for stem cell transplantation. Nat Protoc 8(2):302–309. doi:10.1038/nprot.2013.002
23. Honczarenko M, Le Y, Swierkowski M et al (2006) Human bone marrow stromal cells express a distinct set of biologically functional chemokine receptors. Stem Cells 24(4):1030–1041. doi:10.1634/stemcells.2005-0319
24. Lv FJ, Tuan RS, Cheung KM et al (2014) Concise review: the surface markers and identity of human mesenchymal stem cells. Stem Cells 32(6):1408–1419. doi:10.1002/stem.1681
25. Chandrakanthan V, Yeola A, Kwan JC et al (2016) PDGF-AB and 5-Azacytidine induce conversion of somatic cells into tissue-regenerative multipotent stem cells. Proc Natl Acad Sci USA 113(16):E2306–E2315. doi:10.1073/pnas.1518244113
26. Zhang Y, Cao N, Huang Y et al (2016) Expandable cardiovascular progenitor cells reprogrammed from fibroblasts. Cell Stem Cell 18(3):368–381. doi:10.1016/j.stem.2016.02.001
27. Ball SG, Shuttleworth A, Kielty CM (2012) Inhibition of platelet-derived growth factor receptor signaling regulates Oct4 and Nanog expression, cell shape, and mesenchymal stem cell potency. Stem Cells 30(3):548–560. doi:10.1002/stem.1015
28. Hung SC, Pochampally RR, Chen SC et al (2007) Angiogenic effects of human multipotent stromal cell conditioned medium activate the PI3K-Akt pathway in hypoxic endothelial cells to inhibit apoptosis, increase survival, and stimulate angiogenesis. Stem Cells 25(9):2363–2370. doi:10.1634/stemcells.2006-0686
29. Tao H, Han Z, Han ZC et al (2016) Proangiogenic features of mesenchymal stem cells and their therapeutic applications. Stem Cells Int 2016:1314709. doi:10.1155/2016/1314709
30. Laschober GT, Brunauer R, Jamnig A et al (2011) Age-specific changes of mesenchymal stem cells are paralleled by upregulation of CD106 expression as a response to an inflammatory environment. Rejuvenation Res 14(2):119–131. doi:10.1089/rej.2010.1077
31. Winkler EA, Bell RD, Zlokovic BV (2010) Pericyte-specific expression of PDGF beta receptor in mouse models with normal and deficient PDGF beta receptor signaling. Mol Neurodegeneration 5:32. doi:10.1186/1750-1326-5-32
32. Wu Y, Zhao RC (2012) The role of chemokines in mesenchymal stem cell homing to myocardium. Stem Cell Rev 8(1):243–250. doi:10.1007/s12015-011-9293-z
33. Guo L, Ge J, Zhou Y et al (2014) Three-dimensional spheroid-cultured mesenchymal stem cells devoid of embolism attenuate brain stroke injury after intra-arterial injection. Stem Cells Dev 23(9):978–989. doi:10.1089/scd.2013.0338
34. Baxter MA, Wynn RF, Jowitt SN et al (2004) Study of telomere length reveals rapid aging of human marrow stromal

cells following in vitro expansion. Stem Cells 22(5):675–682. doi:10.1634/stemcells.22-5-675
35. Krampera M, Pasini A, Rigo A et al (2005) HB-EGF/HER-1 signaling in bone marrow mesenchymal stem cells: inducing cell expansion and reversibly preventing multilineage differentiation. Blood 106(1):59–66. doi:10.1182/blood-2004-09-3645
36. Fiedler J, Etzel N, Brenner RE (2004) To go or not to go: migration of human mesenchymal progenitor cells stimulated by isoforms of PDGF. J Cell Biochem 93(5):990–998. doi:10.1002/jcb.20219
37. Ball SG, Shuttleworth CA, Kielty CM (2007) Vascular endothelial growth factor can signal through platelet-derived growth factor receptors. J Cell Biol 177(3):489–500. doi:10.1083/jcb.200608093
38. Boomsma RA, Geenen DL (2012) Mesenchymal stem cells secrete multiple cytokines that promote angiogenesis and have contrasting effects on chemotaxis and apoptosis. PLoS One 7(4):e35685. doi:10.1371/journal.pone.0035685
39. Nuschke A (2014) Activity of mesenchymal stem cells in therapies for chronic skin wound healing. Organogenesis 10(1):29–37. doi:10.4161/org.27405
40. Gong Z, Calkins G, Cheng EC et al (2009) Influence of culture medium on smooth muscle cell differentiation from human bone marrow-derived mesenchymal stem cells. Tissue Eng Part A 15(2):319–330. doi:10.1089/ten.tea.2008.0161
41. Tamama K, Sen CK, Wells A (2008) Differentiation of bone marrow mesenchymal stem cells into the smooth muscle lineage by blocking ERK/MAPK signaling pathway. Stem Cells Dev 17(5):897–908. doi:10.1089/scd.2007.0155